Liquid Crystals
Publication details, including instructions for authors and subscription information:
http://www.informaworld.com/smpp/title~content=t713926090

Study of molecular orientational states of ferroelectric liquid crystals in a surface stabilized geometry

N. Itoh[a]; M. Koden[a]; S. Miyoshi[a]; T. Wada[a]
[a] Central Research Laboratories, SHARP Corporation, Nara, Japan

To cite this Article Itoh, N. , Koden, M. , Miyoshi, S. and Wada, T.(1993) 'Study of molecular orientational states of ferroelectric liquid crystals in a surface stabilized geometry', Liquid Crystals, 15: 5, 669 — 687
To link to this Article: DOI: 10.1080/02678299308036486
URL: http://dx.doi.org/10.1080/02678299308036486

LIQUID CRYSTALS, 1993, VOL. 15, NO. 5, 669–687

Study of molecular orientational states of ferroelectric liquid crystals in a surface stabilized geometry

by N. ITOH*, M. KODEN, S. MIYOSHI and T. WADA

Central Research Laboratories, SHARP Corporation,
2613-1 Ichinomoto-cho, Tenri, Nara 632, Japan

(*Received 28 January 1993; accepted 25 April 1993*)

The molecular orientational states of homogeneously aligned, helix unwinding, chiral smectic C liquid crystals placed in a thin cell (surface-stabilized ferroelectric liquid crystals [SSFLC]) were studied. They were classified by the optical viewing conditions and the relationship between the directions of the chevron layer structure and the surface pretilt. The molecular orientational models of the states were considered and illustrated with regard to the experimental results. The models of molecular orientation give us a total understanding of the orientational states which appear in SSFLCs with parallel rubbing. Furthermore, the effect of the surface pretilt angle on the orientational and optical properties of SSFLCs is discussed.

1. Introduction

Ferroelectric chiral smectic C liquid crystals have great potential for many applications. The homogeneously aligned, helix unwinding state placed in a thin cell (surface-stabilized ferroelectric liquid crystals (SSFLC) [1]) is interesting as a fast optical response, memory switching device. We have studied the smectic layer structure and the molecular orientation of SSFLCs because they must be responsible for the characteristics of SSFLC devices [2–8].

There are two typical classifications of the molecular orientational states. The uniform (U) and twisted (T) states were reported [9, 10]. This classification is based on the optical viewing behaviour when placed between crossed polarizers. The uniform state shows extinction positions, but the twisted state shows only coloration positions without any extinction. Kanbe *et al.* reported the C1 and C2 states [11]. This classification is based on the relationship between the direction of the chevron layer structure and the direction of the surface pretilt. The C1 and C2 states are easily distinguished because the tilting direction of the chevron layer structure is confirmed by the direction of the zig zag defects [12–14], and the direction of the surface pretilt is consistent with the rubbing direction [15]. Figures 1 (*a*) and (*b*) show the C1 and C2 states related with the zig zag defect.

Anderson *et al.* reported on the molecular orientation of a thin layer of a smectic C host [16, 17], using a triangular director profile (TDP). The propagation of plane polarized light through a twisted birefringent layer can be described using the Jones matrix [18, 19]. Anderson *et al.* also derived the relationships between the molecular orientation and the optical properties theoretically, applying the above description to a thin layer of a smectic C phase.

* Author for correspondence.

0267–8292/93 $10·00

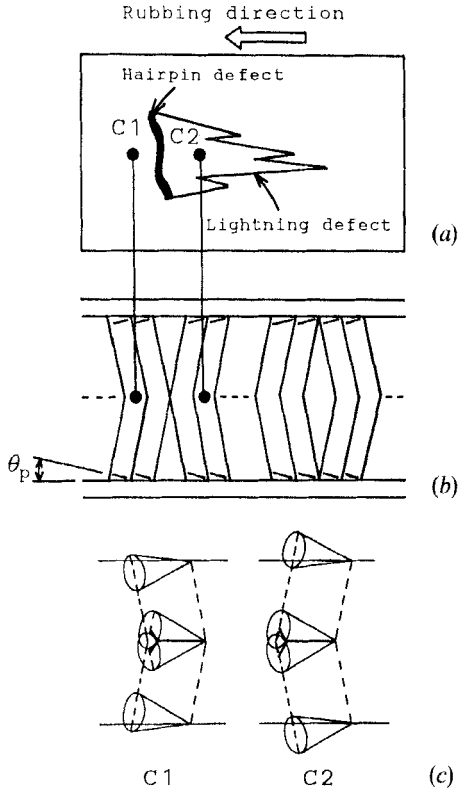

Figure 1. The C1 and C2 states, distinguished by the relationship between the direction of the chevron layer structure and the direction of the surface pretilt, as shown in (*a*) and (*b*). The tilting direction of the chevron layer structure is confirmed by the direction of the zig zag defects, as shown in (*b*). (*c*) The smectic layer models of the C1 and C2 states.

We have previously investigated a number of SSFLC sample cells aligned by various films with parallel rubbing, and reported that the four states, C1U (C1-uniform), C1T (C1-twisted), C2U (C2-uniform), and C2T (C2-twisted), appeared in SSFLC cells [7, 8]. These four states are described by the combination of the above two classifications. Especially, aligned SSFLCs with high pretilts exhibited the three states, C1U, C1T and one C2 state with extinction positions [4, 5]. We proposed the models of these states and simulated the influence of physical parameters on the device properties. A preliminary result on the effect of the surface pretilt angle on the optical properties of SSFLCs was reported [6].

In this study, the molecular orientational states of SSFLCs were analysed by using a polarizing microspectroscope and optical calculations. The models of molecular orientation were constructed, summarizing the orientational states which appear in SSFLCs with parallel rubbing. In addition, the effect of the surface pretilt angle on the molecular orientation and optical properties of SSFLCs is discussed with regard to the simulation based on the molecular orientational models.

2. Experimental

Three ferroelectric liquid crystal (FLC) materials, exhibiting different molecular tilt angles, and six polyimide aligning films exhibiting different pretilt angles, were used in

this study. The FLC materials were CS-1014 supplied by Chisso Co., Ltd., SF-1212 blended at our laboratory, and SCE-8 supplied by E. Merck. The aligning films were PI-X, PSI-A-2101, PSI-A-X018, PI-Z, PSI-A-2001 and PSI-A-X021 supplied by the Chisso Co., Ltd. These aligning films were formed on glass plates with an ITO electrode and an insulating film by spin coating, and were then baked and rubbed.

Thin SSFLC cells (about 1·5 μm) rubbed in a parallel direction were fabricated using silica balls as the spacer, and were filled with the FLC materials. The cells were mounted in a Mettler FP 82 hot stage and positioned between the cross nicol prisms of an Olympus polarizing microscope. The temperature was controlled to within an accuracy of $\pm 0{\cdot}1$°C. The apparent tilt angle θ_{app} was defined as the half-angle between two extinction positions when a square-wave voltage (± 5 V μm^{-1}, 0·5 Hz) was applied. However, such a low frequency electric field changed the alignment of SCE-8 to give the texture with the roof-top lines and stripes [20, 21]. The apparent tilt angle of SCE-8 was measured by applying a square-wave voltage of 1 kHz, thus preventing the texture change, and was defined as the half-angle between two positions where the photodiode indicated the lowest current level. The apparent tilt angles, at room temperature (25°C), of CS-1014, SF-1212 and SCE-8 were approximately 21·0°, 9·5° and 22·0°, respectively. The layer tilt angles were measured using X-ray diffraction [3]. The X-ray profiles, at room temperature, are shown in figure 2. In figure 2, β is the angle between the incident X-rays and the smectic layer normal. The layer tilt angles δ, at room temperature, of CS-1014, SF-1212 and SCE-8 were 18·0°, 9·0° and 19·5°, respectively. Because of the chevron layer structure, the apparent tilt angle θ_{app} is slightly larger than the tilt angle θ, when an electric field is applied, as shown in figure 3. In figure 3, **n** is the director, **p** is the spontaneous polarization vector and $\mathbf{n}_{XZ}$ is the projection of **n** on the boundary XZ plane. E is the electric field applied along the cell thickness direction, $Y$and z represent the perpendicular line of the cone. The relationship between the apparent tilt angle θ_{app} and the tilt angle θ, is expressed as

$$\theta_{app} = \tan^{-1}(\tan\theta \cdot \sec\delta). \tag{1}$$

Using this equation, the tilt angle θ of CS-1014 was determined to be 20·0°, 9·4° for SF-1212, and 21·0° for SCE-8. These parameters are summarized in table 1. The memory angle θ_m was defined as the half-angle between two extinction positions when no field was applied.

Anti-parallel thick cells (about 50 μm) filled with the nematic liquid crystal E-8, supplied by Merck Ltd. were fabricated to measure the pretilt angles of the aligning films. The pretilt angles were determined by the capacitance–magnetic field curves (C–H curves) [22]. The pretilt angles θ_p of these aligning films are shown in table 2. As it is known that the baking temperature affects the pretilt angle [8], the baking temperatures are also shown in table 2. The prepared sample cells in this study are shown in table 3. An Orc polarizing microspectroscope TFM-120CFT was used to measure the transmitted light of small areas, such as the inside of the zig zag defect.

3. SSFLC cell with a high pretilt aligning film

3.1. *Observation*

Figure 4 shows the polarized optical micrographs of the sample used with CS-1014 and the high pretilt aligning film PSI-A-2001 ($\theta_p = 15°$) in the crossed nicol position. The C1 and C2 states are identified on each side of the zig zag defects. The layer normal is parallel to the polarizer in figure 4 (*a*). Figure 4 (*b*) shows the viewing state when the

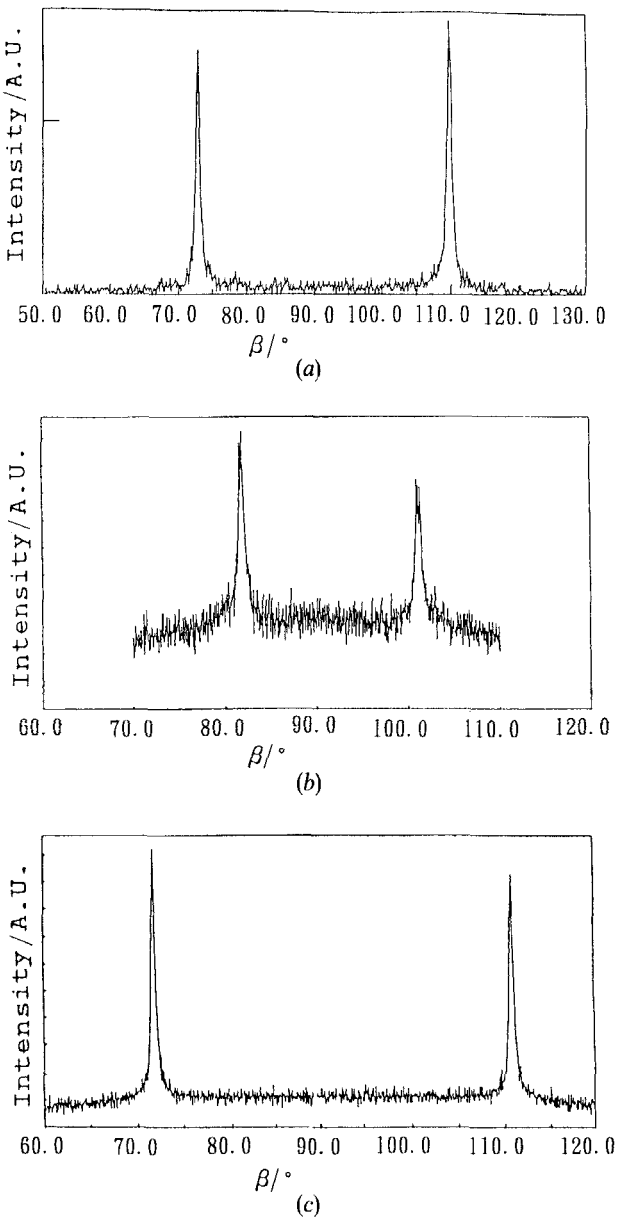

Figure 2. The X-ray profiles of (*a*) CS-1014, (*b*) SF-1212, and (*c*) SCE-8.

sample is rotated from the position of figure 4 (*a*). Figure 4 (*c*) shows the viewing state when the sample is rotated further from the position of figure 4 (*b*). The C2 state of this sample shows extinction positions everywhere. This state is called the C2U state. On the other hand, the C1 state showing extinction positions (C1U), and the state showing only coloration positions with no extinction positions (C1T), are observed. The memory angles of the C1U and C2U states are shown schematically in figure 4. The memory angle of the C1U state is greater than that of the C2U state [figures 4 (*b*) and (*c*)].

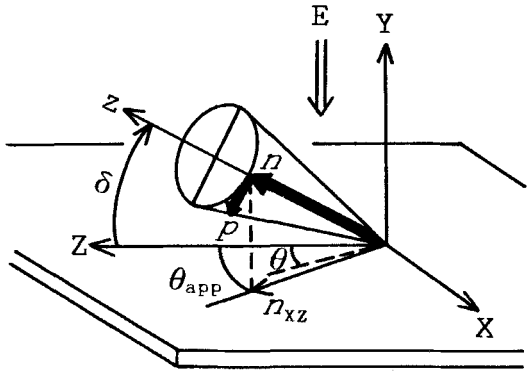

Figure 3. The coordinate system of the tilted layer structure. Here θ is the molecular tilt angle and θ_{app} is the apparent tilt angle.

Table 1. Tilt angles and layer tilt angles of FLC materials at 25°C.

FLC material	Apparent tilt angle/°	Layer tilt angle/°	Tilt angle/°
CS-1014†	21·0	18·0	20·0
SF-1212‡	9·5	9·0	9·4
SCE-8§	22·0	19·5	21·0

† Supplied by Chisso Co., Ltd.
‡ Our blending mixture.
§ Supplied by Merck Ltd.

Table 2. Baking temperatures and pretilt angles of aligning films.

Aligning film†	Baking temperature/°C	Pretilt angle/°
PI-X	200	3
PSI-A-2101	200	6
PSI-A-X018	250	10
PI-Z	250	10
PSI-A-2001	200	15
PSI-A-X021	250	20

† All aligning films were supplied by Chisso Co., Ltd.

Table 3. Prepared sample cell.

	FLC material		
Aligning film	CS-1014	SF-1212	SCE-8
PI-X	●	●	●
PSI-A-2101	●	●	●
PSI-A-X018	●	●	
PI-Z			●
PSI-A-2001	●	●	●
PSI-A-XP21	●	●	

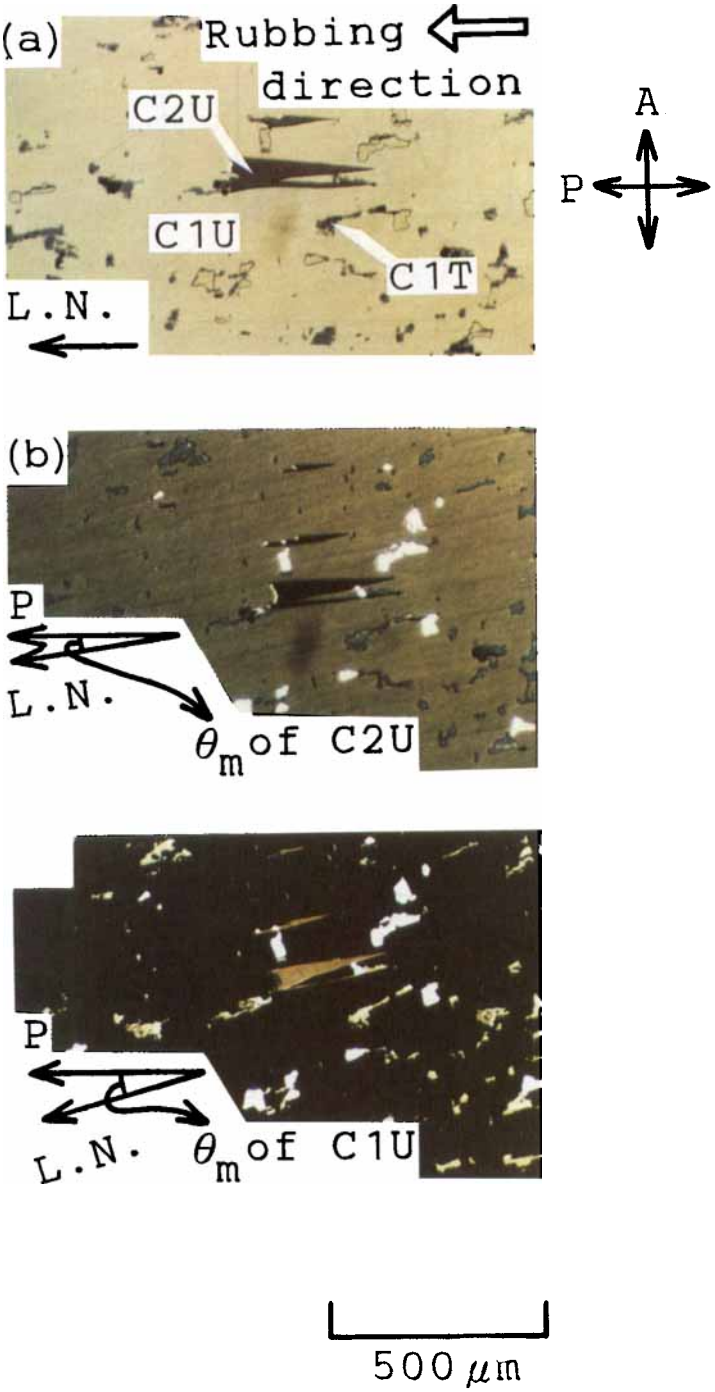

Figure 4. The polarized optical micrographs of the sample used with CS-1014 and the high pretilt aligning film PSI-A-2001. See text for explanation. L.N. denotes the layer normal.

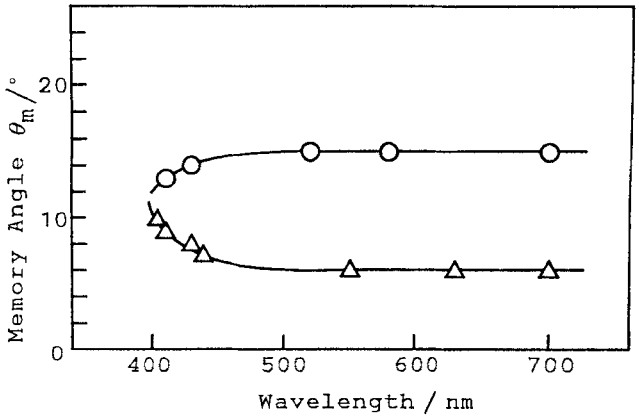

Figure 5. The wavelength dependences of the memory angle of the C1U state (○) and the C2U state (△).

3.2. *Optical properties*

The optical properties of the sample used with CS-1014 and PSI-A-2001, were measured in detail in order to analyse the molecular orientations. The wavelength dependences of the memory angles of the C1U and C2U states are shown in figure 5. The C1U and C2U states exhibit the opposite wavelength dispersion with respect to each other. The transmission spectra of both memory states, the bright and dark states, prepared by applying a pulsed electric field, are shown in figure 6. The transmission spectra indicate that a high contrast ratio is obtained not by the C2U state, but by the C1U state. The large memory angle contributed to a high contrast ratio in this case.

4. Modelling of experimental results

Theoretical calculations are now performed using the experimental results mentioned above.

4.1. *Models of molecular orientation*

The smectic layer models of the C1 and C2 states are shown in figure 1 (*c*). The orientational models of the C1U, C1T and C2U states are shown in figure 7. These states are assumed to switch between two elastically equivalent states for the stable memory effect. The molecules are almost uniformly tilted at one side from the layer normal in the C1U and C2U models. The C1T model is the half splayed state [23–25]. The boundary surfaces in the C2 state do not have wide regions wherein the molecules can exist stably, as shown in figure 1 (*c*). The *c*-directors at the surfaces are almost perpendicular to the substrate in the C2 model with a high pretilt aligning film.

4.2. *Optical simulation*

The transmitted light was calculated using the Berreman 4 × 4 matrix method [26]. We assume the cartesian coordinate systems as shown in figure 8. In figure 8, **n** is the director, **c** is the **c**-director and **p** is the spontaneous polarization vector. It is assumed that the tilt angle θ and the layer tilt angle δ are constant and the azimuthal angle Φ depends only on the cell thickness direction *Y*. The director is expressed as follows;

$$\mathbf{n}(x, y, z) = (\sin\theta\cos\Phi, \sin\theta\sin\Phi, \cos\theta), \tag{2}$$

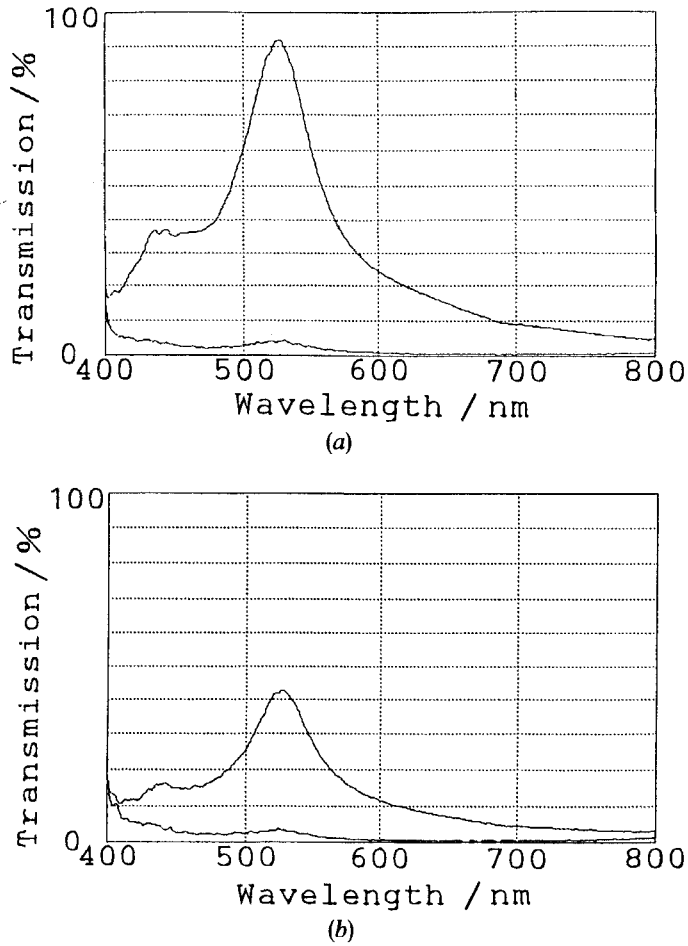

Figure 6. The transmission spectra of the (*a*) C1U and (*b*) C2U memory states. The upper curves represent the bright spectra and the bottom curves represent the dark spectra.

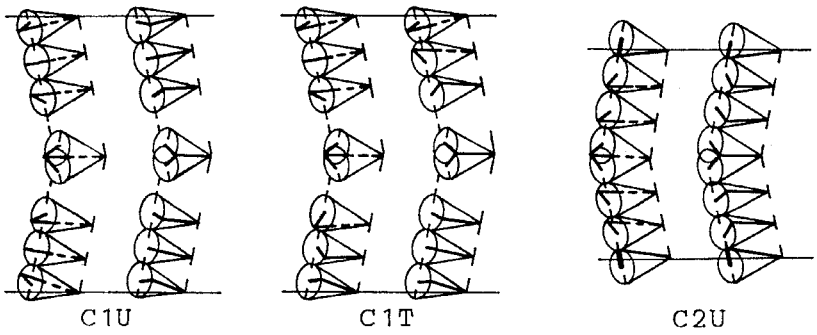

Figure 7. The molecular orientational models of SSFLCs, possessing a chevron layer structure, with a high pretilt aligning film.

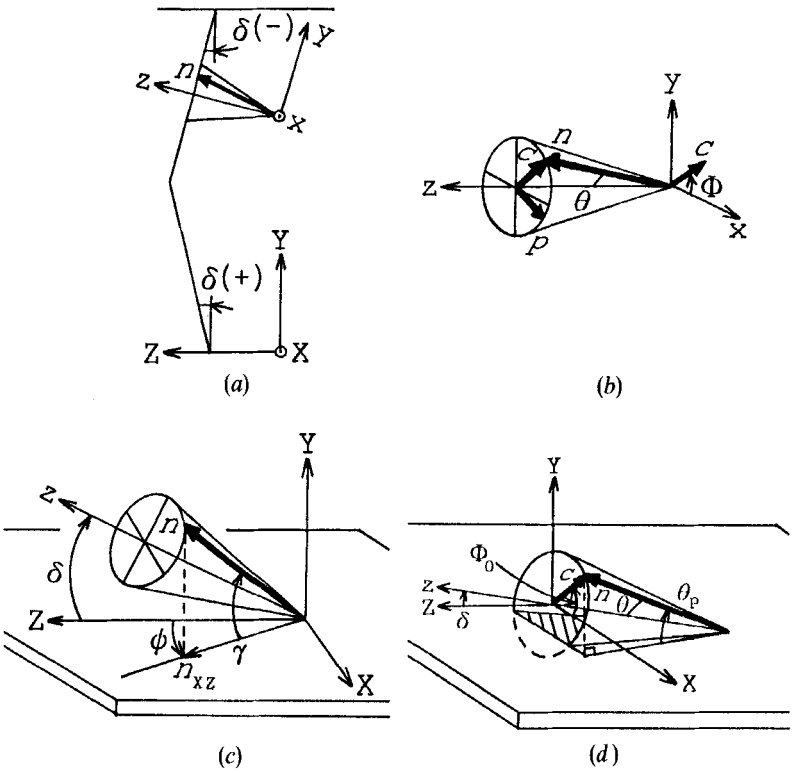

Figure 8. The coordinate systems used for the calculations. Y and Z represent the cell thickness direction and the smectic layer normal, respectively, and z is the perpendicular line of the cone. (*a*) The chevron layer system. (*b*) The cone system. (*c*) The director twist angle ψ and the director tilt angle γ. (*d*) The scheme of the director at the surface.

and

$$\mathbf{n}(X, Y, Z) = \begin{pmatrix} \sin\theta\cos\Phi \\ \sin\theta\sin\Phi\cos\delta - \cos\theta\sin\delta \\ \sin\theta\sin\Phi\sin\delta + \cos\theta\cos\delta \end{pmatrix}. \tag{3}$$

Thus, the twist angle ψ and the tilt angle γ of the director are expressed as

$$\psi = \tan^{-1}\left(\frac{\sin\theta\cos\Phi}{\sin\theta\sin\Phi\sin\delta + \cos\theta\cos\delta}\right), \tag{4}$$

$$\gamma = \sin^{-1}(\sin\theta\sin\Phi\cos\delta - \cos\theta\sin\delta), \tag{5}$$

and are shown in figure 8(*c*). Here, $\mathbf{n}_{XZ}$ is the projection of $\mathbf{n}$ on the boundary XZ plane, as shown previously in figure 3. The dielectric tensor is determined by those two angles. The pretilt angle θ_p is taken at the surface, as shown in figure 8(*d*). Hence, the **c**-director pretilt Φ_0 is expressed by equation (6),

$$\Phi_0 = \sin^{-1}\left(\frac{\tan\delta}{\tan\theta} + \frac{\sin\theta_p}{\sin\theta\cos\delta}\right). \tag{6}$$

It is assumed that Φ_0 at the bottom surface is $\pi/2$ and Φ_0 at the top surface is $-\pi/2$ in the C2 state with a high pretilt aligning film. The azimuthal angle at the chevron interface Φ_{IN} is expressed as

$$\Phi_{IN} = \sin^{-1}(\tan\delta/\tan\theta). \tag{7}$$

It should be noted that the sign of δ is opposite for the C1 and C2 states, and the sign of θ_p is also opposite at the bottom and top surfaces.

For simplicity, it is assumed that Φ changes with Y at a constant rate, ignoring the effect of the polarization field on the elastic deformation [27]. The parameters required for the calculations were obtained experimentally in § 2 and are shown in tables 1 and 2. Other parameters assumed were the cell thickness $d = 1{\cdot}5\ \mu$m, the division number of the liquid crystal layer $N = 300$, and the birefringence $\Delta n = 0{\cdot}15$. The wavelength dispersion of refractive indices [28] was taken into account. In the calculations, it was assumed that the liquid crystal layer, which was sandwiched between two glass plates (refractive index 1·5), was set between two crossed polarizers. The wavelength dependences of the memory angles and the transmission spectra were calculated using the parameters of CS-1014 and PSI-A-2001 ($\theta_p = 15°$). The calculated wavelength dependences of the memory angles are shown in figure 9. Both the C1U and C2U models exhibit the same dispersion as the experimental results. Figure 10 shows the calculated transmission spectra under conditions where the angles between the layer normal and polarizer are the same as the memory angles. The C1U and C2U models show slight transmission in short wavelength regions of the dark states, and show a peak around 500 nm of the bright states. The calculated results are almost consistent with the experimental results, indicating the validity of our orientational models.

5. Effect of pretilt angle on molecular orientations

The orientational models of figure 7 lead us to expect that two states appear in the C2 state with low surface pretilt, because the molecules at the surfaces become easy to move compared to the high pretilt case. The models of these C2 states are shown in figure 11. It is expected that they are the C2U and C2T states. As we introduced in § 1, Anderson *et al.* derived the relationships between the molecular orientation and the optical properties [16, 17]. They did not, however, refer to the effect of the surface pretilt angle.

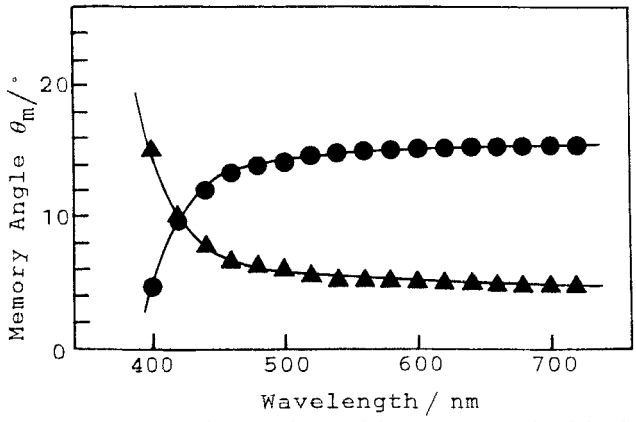

Figure 9. The calculated wavelength dependence of the memory angle of the C1U state (●) and the C2U state (▲).

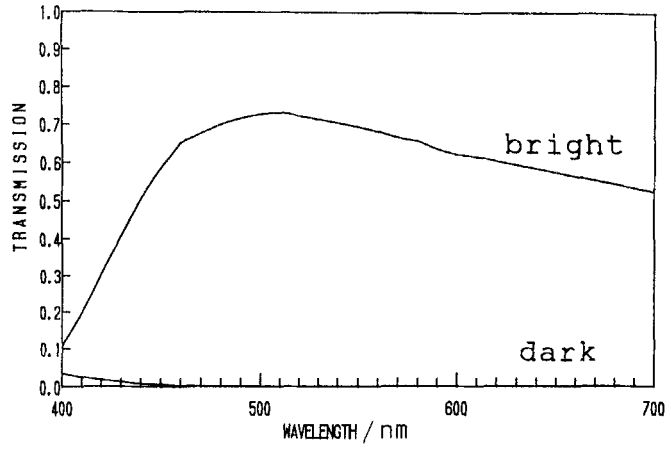

(*a*)

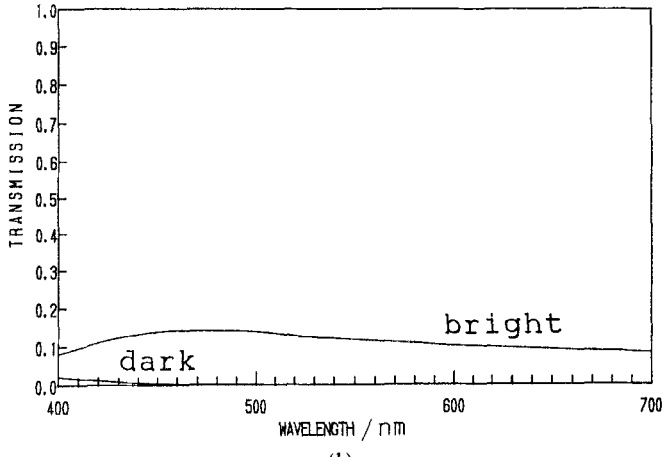

(*b*)

Figure 10. The calculated transmission spectra, of the (*a*) C1U and (*b*) C2U states.

We again experimented in order to prove this hypothesis. The polarized optical micrographs of the sample used with CS-1014 and PI-X ($\theta_p = 3°$) in the crossed nicol position are shown in figure 12. The C1 and C2 states are identified on each side of the zig zag defects. The layer normal is parallel to the polarizer in figure 12 (*a*). Figure 12 (*b*) shows the viewing state when the sample is rotated from the position of figure 12 (*a*). Both the C1 and C2 states show extinction positions. Figure 12 (*c*) shows another area of the sample. Both the C1 and C2 states show only coloration positions without any extinction positions. The C2 state in figure 12 (*c*) is called the C2T state. From figures 4 and 12, it is found that the four states, C1U, C1T, C2U and C2T can appear in SSFLCs with parallel rubbing, and that SSFLCs with high pretilt aligning films show only one state with extinction positions in the C2 state. This type of C2 state is defined as a special case of the C2U state, called the high pretilt C2U state and is shown in figure 11. The C1U and C2U states are interesting from the practical point of view because they show extinction positions.

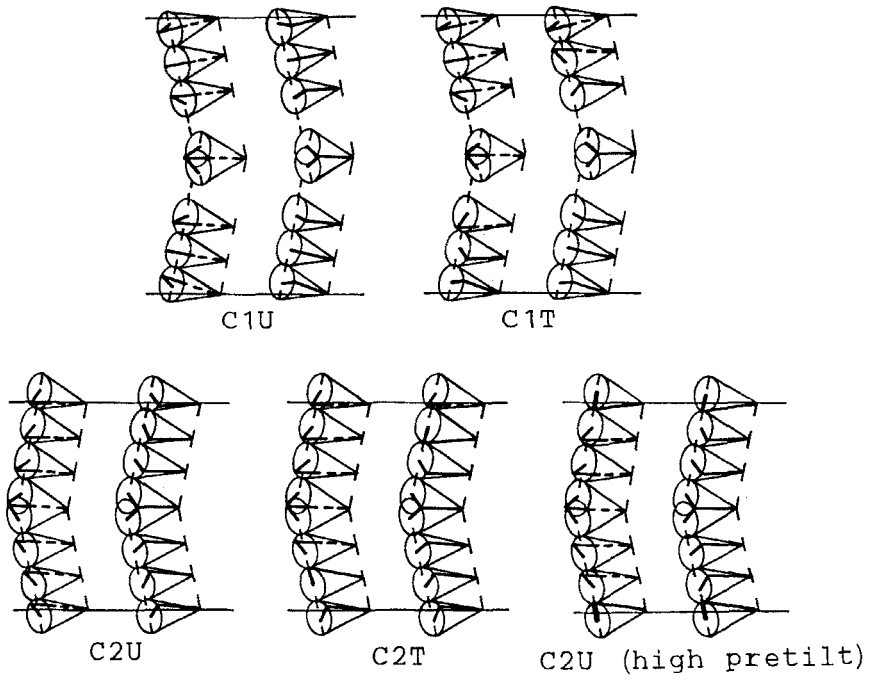

Figure 11. The molecular orientational models of SSFLCs with a chevron layer structure.

5.1. *Surface pretilt dependence of memory angle*

The memory angle of the C1U state is greater than that of the C2U state in the high pretilt sample (figures 4 (*b*) and (*c*)). However, the difference between the memory angles of the C1U and C2U states is very small in the low pretilt sample (figure 12 (*b*)). It is expected that the memory angle depends on the surface pretilt angle from figures 4 and 12.

The temperature dependences of the memory angles of the C1U and C2U states, for all samples, are shown in figure 13. The solid lines in figure 13 represent the apparent tilt angle behaviour. There is little difference in the apparent tilt angles among the samples, indicating the reliability of the data. The memory angles of the C2U state of SSFLC cells prepared using SF-1212, and aligning films except PI-X and PSI-A-2101, could not be measured because the cells showed only the C1 state with slight zig zag defects. According to Kanbe *et al.* [11], it is difficult for the C2 state in SSFLC cells to appear if the tilt angle is small or the surface pretilt angle is large.

The memory angle of the C2U state was almost independent on the pretilt angle. The memory angle of the C1U state in the cases of CS-1014 and SCE-8 strongly depended on the aligning films. On the other hand, the memory angles of the C1U state of SF-1212 were scarcely dependent on the aligning films.

The dependences of the memory angles on the surface pretilt angle were simulated using the models in figures 7 and 11, and are shown in figure 14 with the experimental results at room temperature. In every case, the calculated memory angle is the value for wide visible wavelengths. For every material, good agreement between the simulated and the experimental results was confirmed.

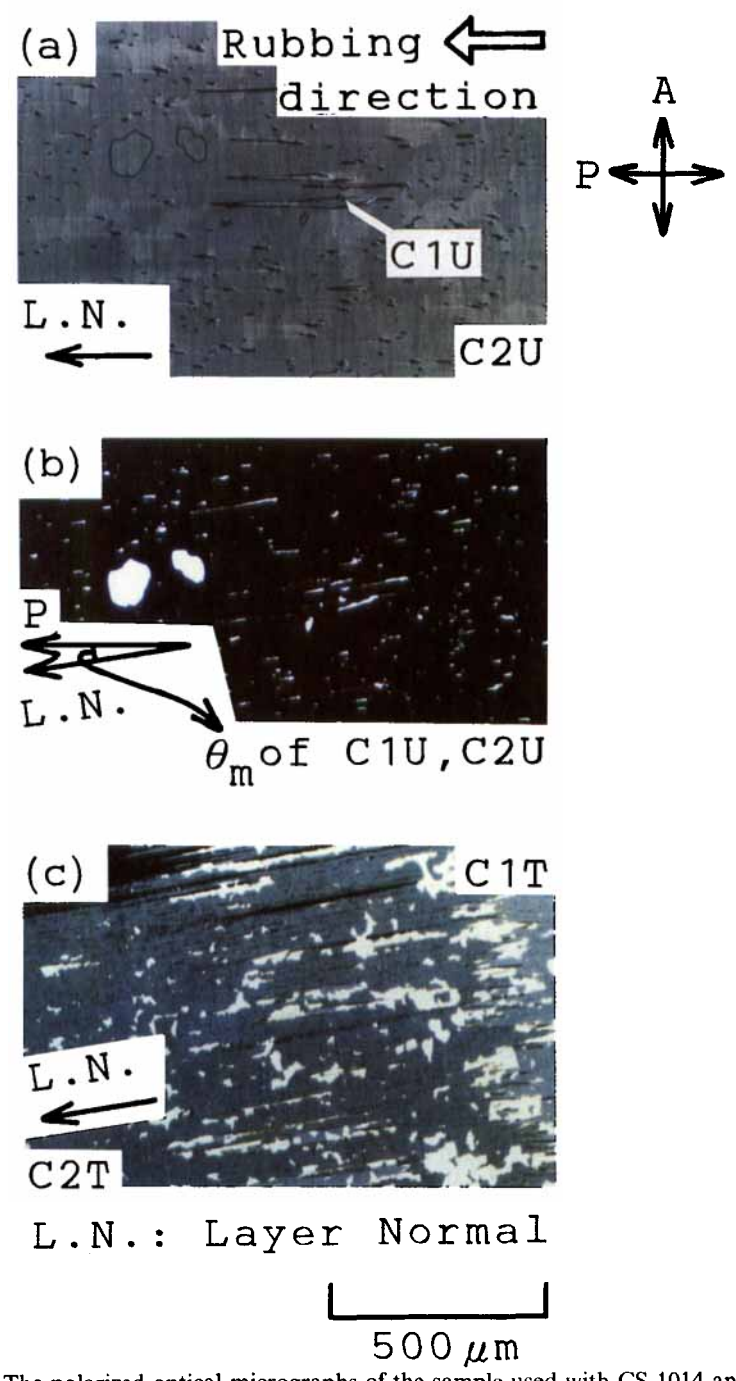

Figure 12. The polarized optical micrographs of the sample used with CS-1014 and the low pretilt aligning film PI-X. See text for explanation of figures.

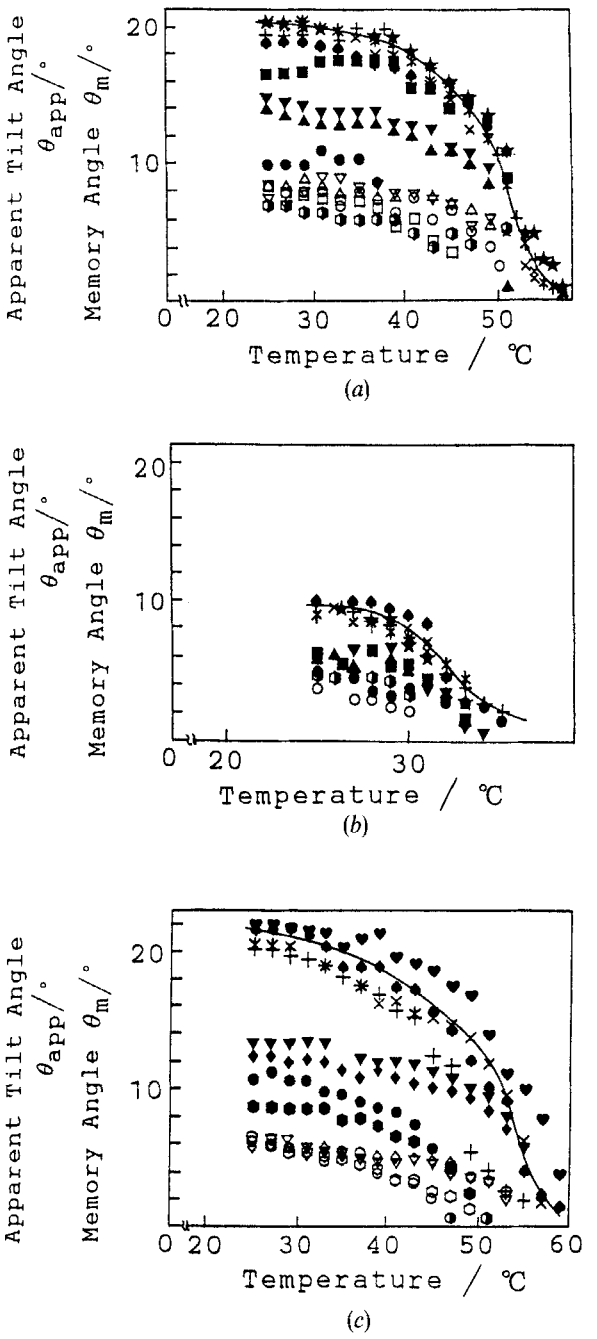

Figure 13. The temperature dependence of the apparent tilt angle (♠, +, ×, ♥, *, ★), the memory angle of the C1U state (⬢, ●, ▲, ◆, ▼, ■) and the C2U state (⬡, ○, △, ◇, ▽, □) with various aligning films (PI-X (♠, ⬢, ⬡), PSI-A-2101 (+, ●, ○), PSI-A-X018 (×, ▲, △), PI-Z (♥, ◆, ◇), PSI-A-2001 (*, ▼, ▽) and PSI-A-X021 (★, ■, □)) for (*a*) CS-1014, (*b*) SF-1212 and (*c*) SCE-8. The lines are the apparent tilt angle behaviour.

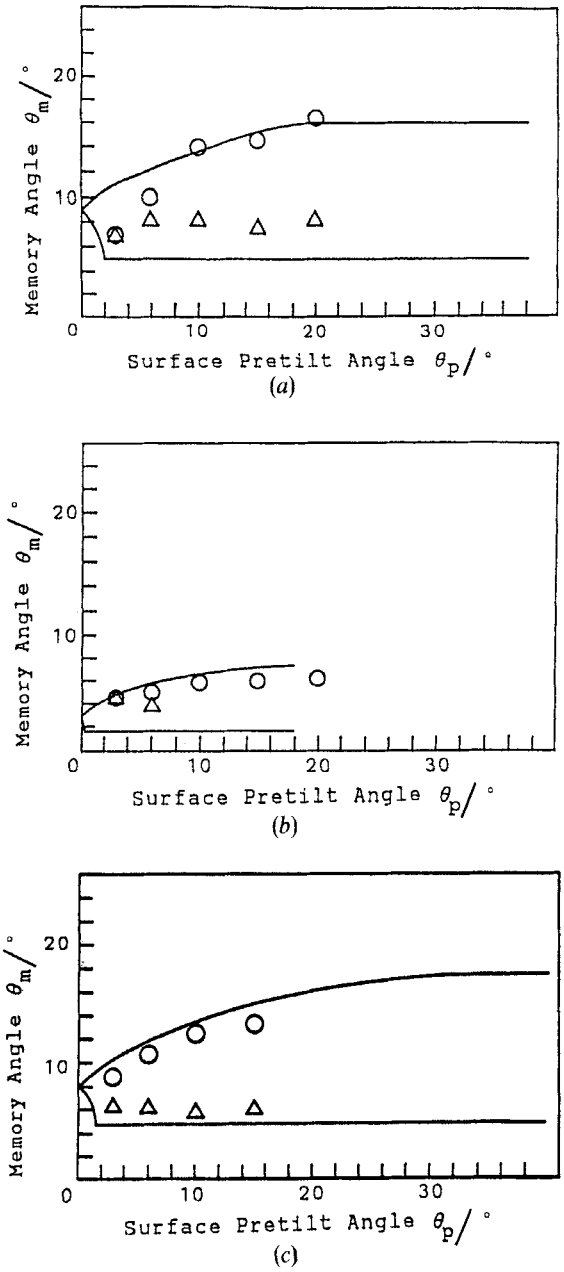

Figure 14. The relationships between the surface pretilt angle and the memory angle of the C1U state (○), and of the C2U state (△) for (*a*) CS-1014, (*b*) SF-1212 and (*c*) SCE-8. The lines are the simulated results.

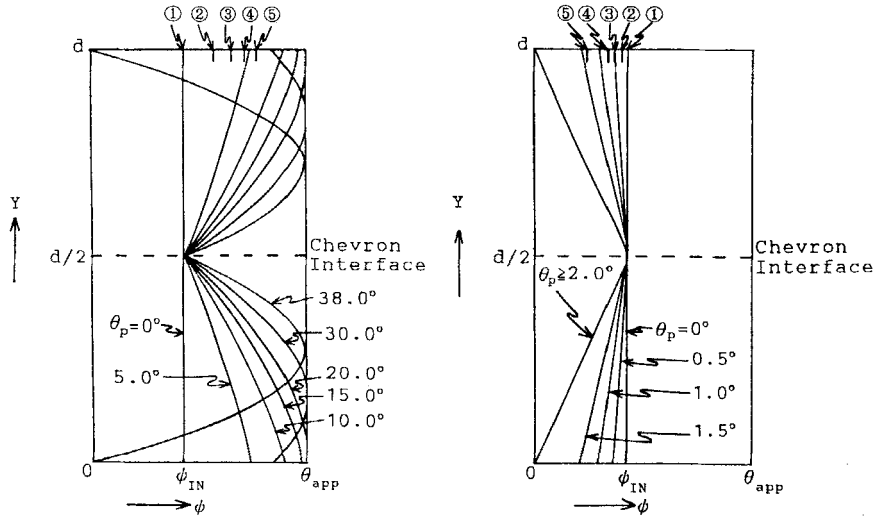

Figure 15. The calculated director profiles and the memory angles for various surface pretilt angles for the (*a*) C1U and (*b*) C2U states. The memory angles are denoted by encircled numerals. In (*a*), 1: $\theta_m(\theta_p=0°)$, 2: $\theta_m(\theta_p=5{\cdot}0°)$, 3: $\theta_m(\theta_p=10{\cdot}0°)$, 4: $\theta_m(\theta_p=15{\cdot}0°)$ and 5: $\theta_m(\theta_p \geqslant 20{\cdot}0°)$. In (*b*), 1: $\theta_m(\theta_p=0°)$, 2: $\theta_m(\theta_p=0{\cdot}5°)$, 3: $\theta_m(\theta_p=1{\cdot}0°)$, 4: $\theta_m(\theta_p=1{\cdot}5°)$ and 5: $\theta_m(\theta_p \geqslant 2{\cdot}0°)$.

5.2. *Analysis using models*

The optical properties mentioned above are now discussed using our models. Whole calculations were performed for CS-1014. In figure 15, the director twist angle ψ is shown as a function of the cell thickness direction Y for various surface pretilt angles in our models, where ψ_{IN} represents ψ at the chevron interface and is expressed as

$$\psi_{IN} = \cos^{-1}(\cos\theta/\cos\delta). \tag{8}$$

The memory angles of each case are indicated simultaneously in figure 15. In figure 16, the calculated transmission spectrum for each case is shown. These figures indicate that the memory angle and the transmission of the bright state depend on the surface pretilt angle. It is found that the memory angle θ_m is determined by the following equation,

$$\theta_m \fallingdotseq (\psi_0 + \psi_{IN})/2, \tag{9}$$

where ψ_0 is ψ at the surface. The memory angle of the C1U state becomes large by increasing the surface pretilt angle and will be saturated at values of θ_{msat} expressed as in equation (10),

$$\theta_{msat} \fallingdotseq (\psi_{IN} + \theta_{app})/2. \tag{10}$$

On the other hand, the memory angle of the C2U state becomes large by decreasing the surface pretilt angle. The results in figure 14 are well explained by our orientational models. However, the memory angle of the C2U state seems to be virtually constant because its surface pretilt dependence is very slight.

6. Summary

The orientational states which appear in SSFLC cells with parallel rubbing are summarized in figure 17, expressed by the **c**-director orientations and the director profiles. The technique of preparing a suitable state is very important not only for

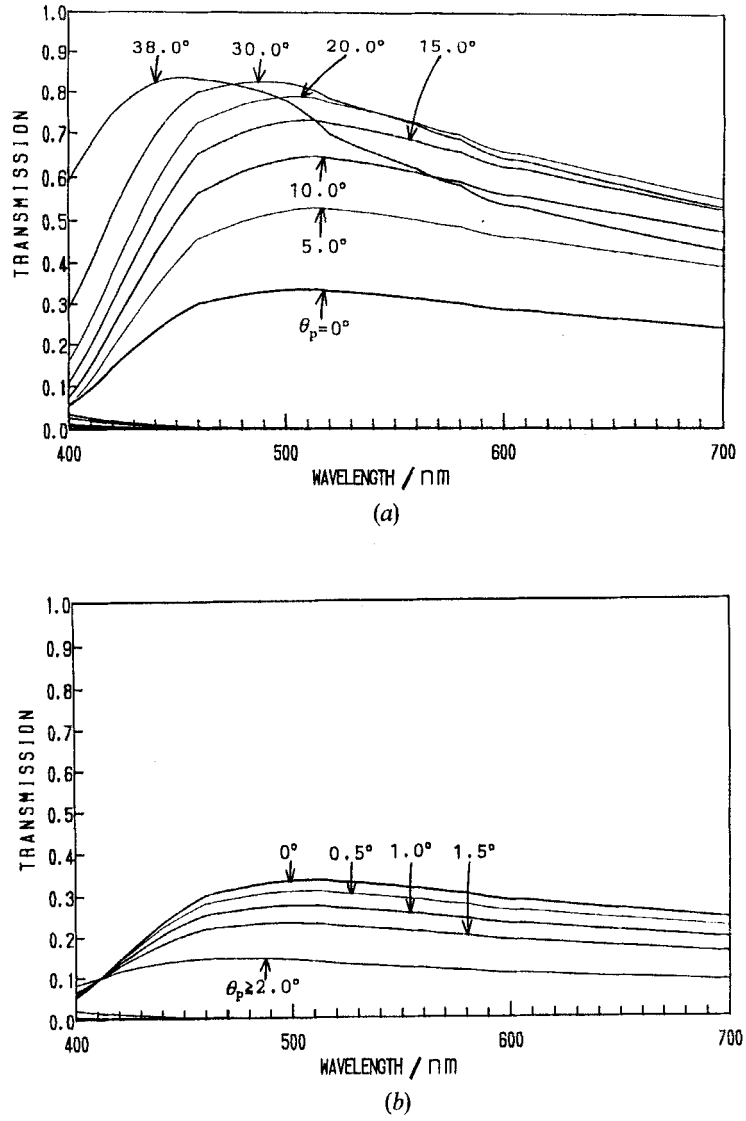

Figure 16. The calculated transmission spectra for various surface pretilt angles of the (*a*) C1U and (*b*) C2U states.

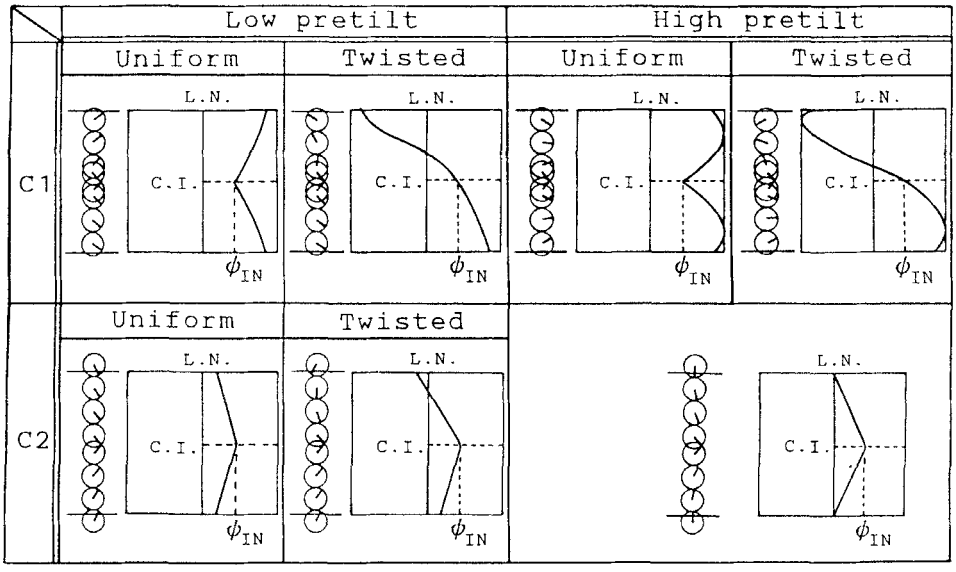

Figure 17. A summary of the orientational states in the SSFLCs with the chevron layer structure.

practical applications, but also to enable reliable experiments. The stability and the optical properties of these states are strongly affected by the surface pretilt angle. An understanding of the effect of the surface pretilt angle is given by our molecular orientational models. However, it is found that differences between the theoretical and experimental results are remarkable in low pretilt regions of figure 14. The behaviour of FLC molecules near the surface, including the pretilt, is more complicated than for nematics. Research to elucidate this problem is needed and is now in progress.

The authors thank Prof. T. Akahane of Nagaoka University of Technology, and Mr A. Tagawa, Mr H. Katsuse and Mr M. Kido of Sharp Corp. for helpful discussions and suggestions.

References

[1] Clark, N. A., and Lagerwall, S. T., 1980, *Appl. Phys. Lett.*, **36**, 899.
[2] Itoh, N., and Nakagawa, K., 1991, *Jap. J. appl. Phys.*, **30**, 335.
[3] Itoh, N., Narutaki, Y., Shinomiya, T., Koden, M., Miyoshi, S., and Wada, T., 1992, *Jap. J. appl. Phys.*, **31**, 1414.
[4] Koden, M., Shinomiya, T., Itoh, N., Kuratate, T., Taniguchi, T., Awane, K., and Wada, T., 1991, *Jap. J. appl. Phys.*, **30**, L1823.
[5] Itoh, N., Koden, M., Miyoshi, S., and Wada, T., 1992, *Jap. J. appl. Phys.*, **31**, 852.
[6] Itoh, N., Kido, M., Tagawa, A., Koden, M., Miyoshi, S., and Wada, T., 1992, *Jap. J. appl. Phys.*, **31**, L1089.
[7] Koden, M., Katsuse, H., Tagawa, A., Tamai, K., Itoh, N., Miyoshi, S., and Wada, T., 1992, *Jap. J. appl. Phys.*, **31**, 3632.
[8] Tagawa, A., Katsuse, H., Tamai, K., Itoh, N., Koden, M., Miyoshi, S., and Wada, T., 1992, *Proceedings Japan Display '92*, 519.
[9] Handschy, M. A., Clark, N. A., and Lagerwall, S. T., 1983, *Phys. Rev. Lett.*, **51**, 471.
[10] Ouchi, Y., Takezoe, H., and Fukuda, A., 1987, *Jap. J. appl. Phys.*, **26**, 1.
[11] Kanbe, J., Inoue, H., Mizutome, A., Hanyuu, Y., Katagiri, K., and Yoshihara, S., 1991, *Ferroelectrics*, **114**, 3.
[12] Clark, N. A., and Rieker, T. P., 1988, *Phys. Rev.* A, *Rap. Commun.*, **37**, 1053.

[13] OUCHI, Y., TAKANO, H., TAKEZOE, H., and FUKUDA, A., 1988, *Jap. J. appl. Phys.*, **27,** 1.
[14] HIJI, N., OUCHI, Y., TAKEZOE, H., and FUKUDA, A., 1988, *Jap. J. appl. Phys.*, **27,** L1.
[15] OKANO, K., and KOBAYASHI, S., 1985, *Application of Liquid Crystals* (Baihukan Press), Chap. 2 (in Japanese).
[16] ANDERSON, M. H., JONES, J. C., RAYNES, E. P., and TOWLER, M. J., 1991, *J. Phys.* D, **24,** 338.
[17] ANDERSON, M. H., JONES, J. C., RAYNES, E. P., and TOWLER, M. J., 1991, *Liq. Crystals*, **10,** 439.
[18] JONES, R. C., 1941, *J. opt. Soc. Am.*, **31,** 493.
[19] RAYNES, E. P., 1987, *Molec. Crystals liq. Crystals*, **4,** 69.
[20] WILLIS, P. C., CLARK, N. A., and XUE, J-Z., 1990, *SID 90 Digest*, p. 114.
[21] RIEGER, H., ESCHER, C., ILLIAN, G., JAHN, H., KALTBEITZEL, A., OHLENDORF, D., RAÖSCH, N., HARADA, T., WEIPPERT, A., and LÜDER, E., 1991, *SID 91 Digest*, p. 396.
[22] SUZUKI, K., TORIYAMA, K., and FUKUHARA, A., 1978, *Appl. Phys. Lett.*, **33,** 561.
[23] CLARK, N. A., RIEKER, T. P., and MACLENNAN, J. E., 1988, *Ferroelectrics*, **85,** 79.
[24] MACLENNAN, J. E., CLARK, N. A., HANDSCHY, M. A., and MEADOWS, M. R., 1990, *Liq. Crystals*, **7,** 753.
[25] ELSTON, S. J., and SAMBLES, J. R., 1990, *Jap. J. appl. Phys.*, **29,** L641.
[26] BERREMAN, D. W., 1972, *J. opt. Soc. Am.*, **62,** 502.
[27] NAKAGAWA, M., and AKAHANAE, T., 1986, *J. phys. Soc. Japan*, **55,** 1516.
[28] KAWAIDA, M., YAMAGUCHI, T., and AKAHANE, T., 1989, *Jap. J. appl. Phys.*, **28,** L1602.